

PSMB8 as a Novel Target for AML Therapy: Uncovering Synergistic Potential with PI3K Inhibitors

AML Tedavisinde Yeni Bir Hedef Olarak PSMB8 ve PI3K İnhibitörleri ile Sinerjik Potansiyelin Belirlenmesi

Onur ATEŞ¹ , Yağmur Kiraz¹ 

¹Department of Genetics and Bioengineering, Faculty of Engineering, İzmir University of Economics, İzmir, Turkey

Abstract

Acute myeloid leukemia (AML) is a bone marrow condition that arises from abnormalities in hematopoietic stem cells due to genetic mutations in progenitor blood cells. These mutations lead to the uncontrolled proliferation of malignant clonal myeloid stem cells. Although extramedullary symptoms such as myeloid sarcomas and leukemia cutis can arise, the main issue continues to be the disturbances in hematologic cell production. Despite the high complete remission rate in elderly patients, a notable number of patients experience relapse within three years. To address this issue, new objectives must be identified. In a previous study, PSMB8 drew our attention due to its elevated expression levels in AML patients exhibiting lower survival rates compared to those with reduced expression levels. PSMB8 was used for drug repurposing studies by performing in silico drug screening, an ADMET analysis which is followed by Molecular Dynamics (MD) simulations. Three ligand molecules were identified as potential treatment options for AML which were Adozelesin, Fiduxosin and Omipalisib. Omipalisib is known as a PI3K/mTOR inhibitor which was taken our attention for cytotoxic analysis due to overexpression of PI3K/mTOR pathway proteins in AML development. In the subsequent phase, we assessed the cytotoxicity of Omipalisib in comparison to ONX-0914, an inhibitor of PSMB8, in the HL60 cell lines. This research indicated that PSMB8 could be a possible target for Acute Myeloid Leukemia and that a potential medication can be utilized for targeted treatment.

Keywords: Omipalisib, ONX-0914, AML, PI3K/mTOR, PSMB8, Proteasome

Öz

Akut miyeloid lösemi (AML), progenitör kan hücrelerindeki genetik mutasyonlar nedeniyle hematopoetik kök hücrelerde meydana gelen düzensizliklerden kaynaklanan bir kemik iliği hastalığıdır. Bu mutasyonlar, malign klonal miyeloid kök hücrelerin kontrolsüz çoğalmasına yol açar. Miyeloid sarkomlar ve lösemi kutisi gibi ektramedüller belirtiler ortaya çıkabilse de, temel sorun hematolojik hücre üretimindeki bozulmalardır. Yaşlı hastalarda tam remisyon oranı yüksek olmasına rağmen, önemli sayıda hasta üç yıl içinde nüks yaşamaktadır. Bu sorunun üstesinden gelmek için yeni hedeflerin belirlenmesi gerekmektedir. Önceki çalışmamızda, AML hastalarında PSMB8'in yüksek ekspresyon seviyeleri göstermesi ve düşük ekspresyon seviyelerine sahip hastalara kıyasla daha düşük sağkalım oranları ile ilişkilendirilmesi dikkatimizi çekmiştir. Daha önceki çalışmamızda, PSMB8 hedef alınarak sanal ilaç taramaları, ADMET analizi ve ardından Moleküler Dinamik (MD) simülasyonları gerçekleştirilmiştir. Bu çalışmalar sonucunda AML tedavisi için üç potansiyel ilaç adayı belirlenmiştir: Adozelesin, Fiduxosin ve Omipalisib. PI3K/mTOR inhibitörü olarak bilinen Omipalisib, AML gelişiminde PI3K/mTOR yolak proteinlerinin aşırı ekspresyon göstermesi nedeniyle sitotoksitesite analizi için dikkatimizi çekmiştir. Sonraki aşamada, HL60 hücre hattında Omipalisib'in sitotoksitesitesi, PSMB8 inhibitörü olan ONX-0914 ile karşılaştırılmıştır. Bu araştırma, PSMB8'in Akut Myeloid Lösemi için olası bir hedef olabileceğini ve potansiyel bir ilacın hedefli tedavi için kullanılabileceğini gösterdi.

Anahtar Kelimeler: Omipalisib, ONX-0914, AML PI3K/mTOR, PSMB8, Proteazom

I. INTRODUCTION

Acute myeloid leukemia (AML) is a bone marrow disorder stemming from genetic abnormalities in hematopoietic stem cells, leading to malignant clonal expansion of myeloid precursors. While extramedullary manifestations such as myeloid sarcomas and leukemia cutis may occur, the primary pathology involves dysregulated hematopoiesis. In most cases, AML arises from chromosomal aberrations or gene mutations, although the exact mechanism remains unclear. Although some instances have been linked to prior chemotherapy or chemical

exposure, these represent exceptions rather than the predominant cause. Recognizing these genetic mutations is essential for assessing patient risk and guiding appropriate treatment approaches [1].

Acute myeloid leukemia (AML) represents the most common type of acute leukemia among adults, with its incidence rising progressively in older populations. The standard induction chemotherapy regimen, which includes a combination of anthracycline and cytarabine, has been established over the past several decades and remains the primary treatment approach in clinical practice [2]. Whereas at least 85% of identified patients under 60 show a positive response to chemotherapy induction and reach complete remission, a notable proportion relapse within three years [3]. The incorporation of molecularly targeted therapies has led to the use of multidrug regimens in combination with hematopoietic stem cell transplantation (HSCT), achieving a five-year survival rate of approximately 25% among patients [4]. The prognosis of AML is considerably poorer in elderly patients and those who are not fit for standard induction chemotherapy, resulting in a median survival of between 5 and 10 months, with a mere 5% of individuals surviving beyond five years [5]. The classification of acute myeloid leukemia (AML) has evolved from just depending on blast percentage to a broader method that includes cytogenetic and molecular indicators. Diagnosis generally necessitates the presence of more than 20–30% myeloid blasts in the blood or bone marrow or the identification of specific genetic abnormalities. At this point, a comprehensive assessment involving morphology, flow cytometry, and genomic analysis is crucial. The two primary classification systems, WHO and ICC, show slight differences; for instance, ICC requires a minimum of 10% blasts in cases with recurring genetic abnormalities, whereas WHO offers more flexibility. Furthermore, ICC established a category for patients exhibiting 10-19% blasts to expand treatment alternatives. Although there are slight variations, both categorizations highlight the significance of molecular and cytogenetic profiling for precise prognosis and treatment coordination in AML. Acute myeloid leukemia requires immediate diagnosis and frequently arises as an urgent medical condition. Although early symptoms may be nonspecific, patients typically show various indicators associated with immunosuppression, myelosuppression (like severe anemia or thrombocytopenia), and leucocytosis, indicating a potential hematological malignancy [6].

The immunoproteasome enhances protein degradation, generating antigenic peptides that are subsequently presented by major histocompatibility complex class I (MHC-I). The 26S proteasome, responsible for breaking down polyubiquitinated proteins, is composed of a 20S core proteasome coupled with 19S regulatory subunits [7]. The 20S core proteasome is composed of

seven α -type subunits that form a gating mechanism, while its seven β -type subunits serve as the proteolytic active site [8]. The beta type-8 proteasome subunit (PSMB8), known as LMP7 or $\beta 5i$ [9], typically serves as a subunit of the immunoproteasome, activated by TNF- α and IFN- γ [10]. Unlike the conventional proteasome, the immunoproteasome demonstrates enhanced chymotrypsin-like and trypsin-like enzymatic activity, facilitating the production of antigenic peptides for MHC-I presentation [11]. The expression of this immunoproteasome affects cell metabolism, immune regulation, and differentiation. Mutations in PSMB8 have been associated with disorders such as autoinflammation and lipodystrophy in humans, highlighting its function in sustaining dynamic equilibrium [12]. Moreover, PSMB8 inhibits neovascularization in glioma cells through the modulation of the ERK1/2 and PI3K/AKT signaling pathways [13].

Research has established links between the expression of the PSMB8 gene and acute myeloid leukaemia (AML). Analysis of AML datasets highlights a positive correlation between increased PSMB8 levels and the upregulation of galectin-9 (Gal-9), a molecule also highly expressed in AML. This suggests that both play a synergistic role in cellular signaling, survival, and the progression of AML [14]. Another study demonstrated that PSMB8 expression is elevated in AML and strongly correlates with HCP5, a long non-coding RNA found within the HLA Complex P5. Interestingly, silencing HCP5 led to a significant reduction in PSMB8 levels, while its expression remained high in cells with HCP5 overexpression. Furthermore, it appears that the activation of the PI3K/AKT pathway in AML is influenced by HCP5's regulation of PSMB8. Consequently, the activation of PI3K/AKT via PSMB8 in AML is suggested to play a role in driving tumor progression [15]. In addition to these studies, our group have previously conducted an *in silico* analysis concerning PSMB8 in AML for drug repurposing [16]. In our prior research, we explored the essential survival genes within the Cancer Genome Atlas (TCGA) and the LAML (Acute Myeloid Leukemia) dataset using the GEPIA (Gene Expression Profiling Interactive Analysis) tool [17]. Of all the genes associated with survival outcomes, PSMB8 was recognized as a notable candidate in the LAML dataset, drawing from results of earlier studies. With extensive findings, our interest was taken on PSMB8 as a potential target for AML for drug repurposing study [17].

Drug repurposing is among the most commonly employed methods for discovering new uses for medications that have already been approved [18]. This method seeks to significantly reduce both the expenses and duration of research [19]. Drug repurposing initiatives have demonstrated greater efficiency, reduced risk, and cost-effectiveness compared to traditional drug development and discovery methods

[20]. By leveraging repurposed drugs that have already been tested in humans, we gain a more thorough understanding of the drug's pharmacokinetics, pharmacodynamics, dosage, metabolic profiles, molecular pathways, mechanism of action, and a host of other target interactions. As a result, that may reduce the necessity for further research into the pharmacokinetics and toxicity profiles of the medication.

In a previous study conducted by our team, we identified three potential drug candidates for AML treatment: Adozelesin, Fiduxosin, and Omipalisib. Among three drug molecule, various filters have let us with the only available Omipalisib agent which is also a PI3K/mTOR inhibitor that have been found to have strong interactions with PSMB8. Additionally, since the PI3K/mTOR pathway is known to be overly active in AML patients [21], Omipalisib would be well suited to target the PI3K/mTOR pathway as well as being a repurposed drug against PSMB8. On the other side, PSMB8 has known inhibitor molecule as called ONX-0914. In our study, we explored the cytotoxic effects of these drugs on AML cell line HL60 through both individual and combinational treatment approaches. Therefore we have explored for the first time in the literature that PSMB8 could actually be an AML-related novel molecule and it has a potential to be targeted through a drug repurposing approach.

II. MATERIAL AND METHODS

2.1. Cell Growth Conditions

To evaluate the in vitro effectiveness of the drugs, human cell lines were utilized. For this purpose, HL60 cell lines were chosen for testing the selected drugs on AML. HL60 cells were cultured according to standard protocols, using RPMI-1640 medium enriched with 10% Fetal Bovine Serum (FBS) and 1% penicillin/streptomycin, as previously outlined [22].

2.2. MTT Assay

In order to assess cytotoxic effects of ONX-0914 and Omipalisib on the HL60 cell lines, MTT assay was employed. Total number of 1×10^4 cells/well were plated into 96 well plates with various concentrations. After 48 and 72 hours of incubation, MTT reagent with a volume of 20 μ l/well was added to wells and incubated for an additional 4 hours at 37 °C. After this period, the supernatants were gently discarded, and DMSO with volume of 100 μ l used to dissolve the leftover formazan crystals. The plates were subsequently incubated for another 30 minutes at 37 °C. Ultimately, the optical density (OD) readings were recorded [23].

2.3. Cell Growth Curve

The IC₅₀ values determined for ONX-0914 and Omipalisib were tested against HL60 to determine cytotoxic effects with trypan blue staining. 3×10^5

cells/ml were seeded in 6 well plate and incubated for 72 hours and at 48 and 72th hour, samples collected and counted with trypan blue 3 times/sample. The data was using to creation of growth curve, with and absence of the selected drugs [24].

2.4. Flow Cytometry

To evaluate apoptosis using Flow Cytometry, HL60 cells were grown in a 6-well plate with a concentration of 3×10^5 cells/ml, cells treated with drugs for 48 and 72 hours. Subsequently, 1×10^6 cells were gathered, washed two times with PBS, and the pellet was resuspended in 100 μ l of binding buffer. Subsequently, 5 μ l of Annexin APC was introduced to the binding buffer and pellet mixture, followed by the addition of 10 μ l of PI to the mixture after a 10-minute interval. The mixture was kept at room temperature, in pitch dark conditions, for 15 minutes, after which 400 μ l of binding buffer was added. Flow cytometry was then employed to analyze the stained cell lines [25].

2.5. Western Blot

To evaluate apoptosis, a western blot was conducted by measuring the alterations in the expression of PARP and β -Actin, which served as a control. Cell groups were initially exposed to the specified drug concentrations for 48 and 72 hours. Following treatment, cell pellets were harvested, and protein concentrations were determined using the BSA Protein Assay Kit, in accordance with the provided protocol. For the running procedure, a 10% SDS gel was used. The samples were prepared with 5X Loading buffer featuring 100mM β -Mercaptoethanol (BME), 1% Bromophenol blue, 50% Glycerol, SDS 8%, Tris-Cl (250mM, pH 6.8), and H₂O loaded into each well. The gel inserted into the Biorad western blot system and voltages were set to compete the run. The membrane transfer then was conducted using the Biorad Transblot - Turbo Transfer system. For immunodetection, PARP and β -Actin antibodies were prepared following their established protocols. Finally for chemiluminescent detection, ECL substrate is used to incubate the membrane followed by imaging [26].

2.6 Statistical Analysis

All the statistical analysis were done by using GraphPad Prism software (v10.3.1). All data obtained from cytotoxic assays performed through this study. Data expressed as mean \pm SD and Two-way ANOVA test was applied for multiple comparison. Statistical significance level was accepted as $p < 0.05$ (*), $p < 0.01$ (**), $p < 0.001$ (***) and $p < 0.0001$ (****).

III. RESULTS AND DISCUSSION

3.1. Cytotoxic Impact of ONX-0914 and Omipalisib on the HL60 Cells

Omipalisib was previously discovered through molecular docking and dynamics studies and selected for evaluation on the AML cell line, HL60, in

comparison with ONX-0914 to assess cytotoxic effects. To achieve this, every drug was applied separately to

the HL60 cell line and incubated for 48 and 72 hours, after which analysis was conducted using MTT assays.

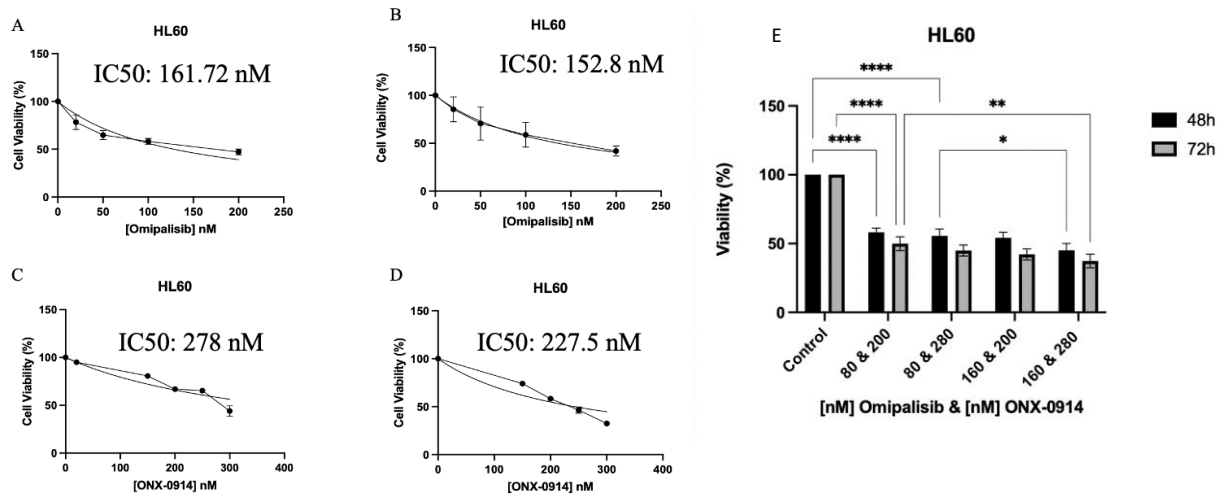


Figure 1. The effects of Omipalisib at 48h (A) and 72h of treatment (B) ONX-0914 at 48h (C) and 72h of treatment (D) on cell viability of HL60 cells. IC50 values were calculated based on MTT assay cell counting measures for each treatment. (E) The effects of combinational treatment of Omipalisib and ONX-0914 at 48 and 72h of treatments on HL60 cells. The viabilities were calculated based on MTT assay cell counting measures for each treatment. Each experiment was conducted as triplicates and error bars represent SD values.

The results showed that, in comparison to ONX-0914, Omipalisib demonstrated greater efficacy, with IC50 values recorded at 161.7nM and 152.8nM for the 48 and 72-hour marks as seen in figure 1A and figure 1B, while IC50 values for ONX-0914 were 277.7nM and 227.5nM as seen in figure 1C and figure 1D.

After administering individual doses of Omipalisib and ONX-0914, combination therapies were implemented. The selected concentrations were 80 nM and 160 nM for Omipalisib, and 200 nM and 280 nM for ONX-0914, based on their IC50 values. Omipalisib had IC50 values of 161 nM and 153 nM, which were very close; therefore, 160 nM was chosen. Additionally, 80 nM was selected to minimize toxicity when combined with ONX-0914. ONX-0914 had IC50 values of 278 nM and 227.5 nM, so 280 nM was chosen for simplicity in calculations, along with 200 nM. Using these concentrations, four distinct combinations were formed: 80nM Omipalisib with 200nM ONX-0914, 160nM Omipalisib with 200nM ONX-0914, 80nM Omipalisib with 280nM ONX-0914, and 160nM Omipalisib with 280nM ONX-0914. Utilizing these concentrations, an MTT assay was conducted over 48 and 72 hours (Figure 1E). Within 48 hours, the sole combination of 160nM Omipalisib and 280nM ONX-0914 reduced viability by 50%, which corresponds to 43.5% viability. Conversely, after 72 hours, the viabilities were found to be 46.5%, 43.3%, 42.2%, and 34.0% respectively. This leads to the most efficient combination of 160nM Omipalisib and 280nM ONX-0914

3.2. Growth Curves Revealed Anti-Proliferative Effects of ONX-0914 and Omipalisib on the HL60 cells

To assess the anti-proliferative effects of Omipalisib and ONX-0914 on HL60 cells, trypan blue cell counting was conducted using specific concentrations for both drugs. Omipalisib was tested at 80 and 160 nM, while ONX-0914 was tested at 200 and 280 nM. Cell counting with trypan blue was performed at 48 and 72 hours for every treatment group, in addition to a control group. In addition to single doses, combination therapies were utilized to assess the antiproliferative impacts of medications on HL60. As shown in Figure 2A, the untreated control group exhibited significant proliferation at both 48 and 72 hours, consistent with the expected growth of HL60 cells under normal conditions. In contrast, cells treated with 80 nM Omipalisib exhibited a noteworthy decrease in proliferation, with further decline observed at 160 nM. This dose-dependent decrease highlights Omipalisib's ability to successfully inhibit cell growth over time.

Similarly, Figure 2B shows the anti-proliferative effects of ONX-0914. The control group again exhibited substantial proliferation, while cells treated with 200nM ONX-0914 displayed reduced growth. The most notable suppression was observed at 280 nM, where cell proliferation was blocked. Notably, the decrease in cell count from 48 to 72 hours in the high concentration group suggests that ONX-0914's efficacy may increase with longer exposure.

In combinational therapies, in most instances, viability diminishes as the concentration of a medication rises. For treatments of 48 hours, the average viable cell counts were computed as 0.35×10^6 cells/ml, 0.28×10^6 cells/ml, 0.31×10^6 cells/ml and 0.16×10^6 cells/ml

based on the established treatment groups. After 72 hours of treatments the viability levels declined to 0.28×10^6 cells/ml, 0.13×10^6 cells/ml, 0.225×10^6 cells/ml and 0.09×10^6 cells/ml as seen in Figure 5.

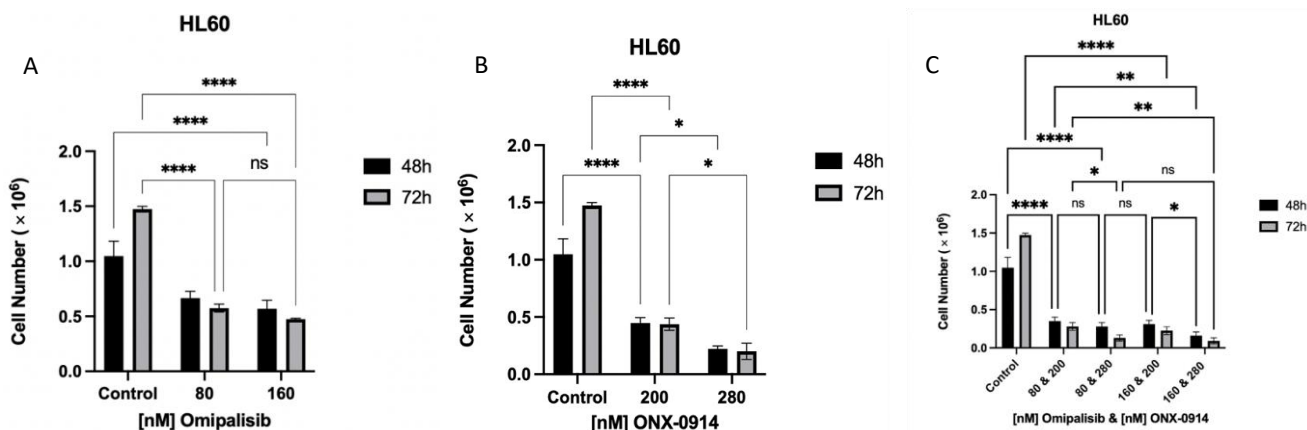


Figure 2. (A) Evaluation of cell viability and proliferation in HL60 cells using Trypan Blue after Omipalisib treatment for 48 and 72h. (B) Evaluation of cell viability and proliferation in HL60 cells using Trypan Blue after ONX-0914 treatment for 48 and 72h. (C) Evaluation of cell viability and proliferation in HL60 cells using Trypan Blue after ONX-0914 and Omipalisib treatment for 48 and 72h. Cell samples were collected at 48 and 72 hours and counted as triplicates. Error bars represent the SD values

In summary, both Omipalisib and ONX-0914 demonstrated dose- and time-dependent actions that reduce the proliferation of HL60 cells. Nevertheless, increased doses of ONX-0914 led to a more significant reduction in cell viabilities than Omipalisib. These findings support the potential therapeutic applications of these drugs in targeting myeloid leukemia cells.

3.3. Flow Cytometry Revealed the Induced Apoptosis in Response to ONX-0914 and Omipalisib Treatment on HL60 cells

To assess the apoptotic effects of the chosen drug, Omipalisib, the Annexin/PI staining technique was utilized. The experiment spanned 72 hours, with measurements gathered at the 48th and 72nd hour intervals using a flow cytometer. Throughout the study, HL60 cells received individual treatments of 80nM and 160nM Omipalisib at specified time intervals. As a positive control, HL60 cells were exposed to 100nM doxorubicin. Annexin/PI staining demonstrated that doses of 80 nM and 160 nM of Omipalisib as shown in Figure 3 led to a steady rise in apoptosis. Additionally, these results validated the consistency of the doses established via the MTT assay. Omipalisib induced a time-dependent increase in apoptosis, with no significant difference between 80 nM and 160 nM at 48 hours, but a significant apoptotic increase at 160 nM by 72 hours ($p < 0.05$). This suggests that Omipalisib's pro-apoptotic effect intensifies over time rather than being purely dose-dependent.

To compare Omipalisib and evaluate the effect of PSMB8 inhibition on cell viability, ONX-0914 was

chosen for treatment at concentrations of 200nM and 280nM. The study was carried out over 72 hours, with data gathered at the 48th and 72nd hour marks using a flow cytometer as seen in Figure 4.

ONX-0914 induced dose- and time-dependent apoptosis, with 200 nM significantly increasing apoptosis compared to the control, and 280 nM leading to an even greater effect ($p < 0.0001$). The difference between 200 nM and 280 nM was significant at both 48 and 72 hours, confirming that higher ONX concentrations further enhance apoptosis as seen in Figure 4.

Ultimately, the combinations identified previously were employed to identify apoptotic cell populations following treatments for 48 and 72 hours. Combination therapy with 80 nM Omi & 200 nM ONX and 160 nM Omi & 200 nM ONX led to significant increases in apoptosis, with stronger effects observed at 72 hours. The most potent combinations were 80 nM Omi & 280 nM ONX and 160 nM Omi & 280 nM ONX, where apoptosis levels approached 70-77%, indicating a synergistic effect of the higher ONX concentration as seen in Figure 5.

In conclusion, either single or combined use of Omipalisib and ONX-0914 can be proposed to use in the treatment of AML. The findings indicate that blocking PSMB8 may serve as a viable treatment option for AML. Combined therapies demonstrate heightened toxicity across all groups, achieving peak levels of apoptosis during the treatment process.

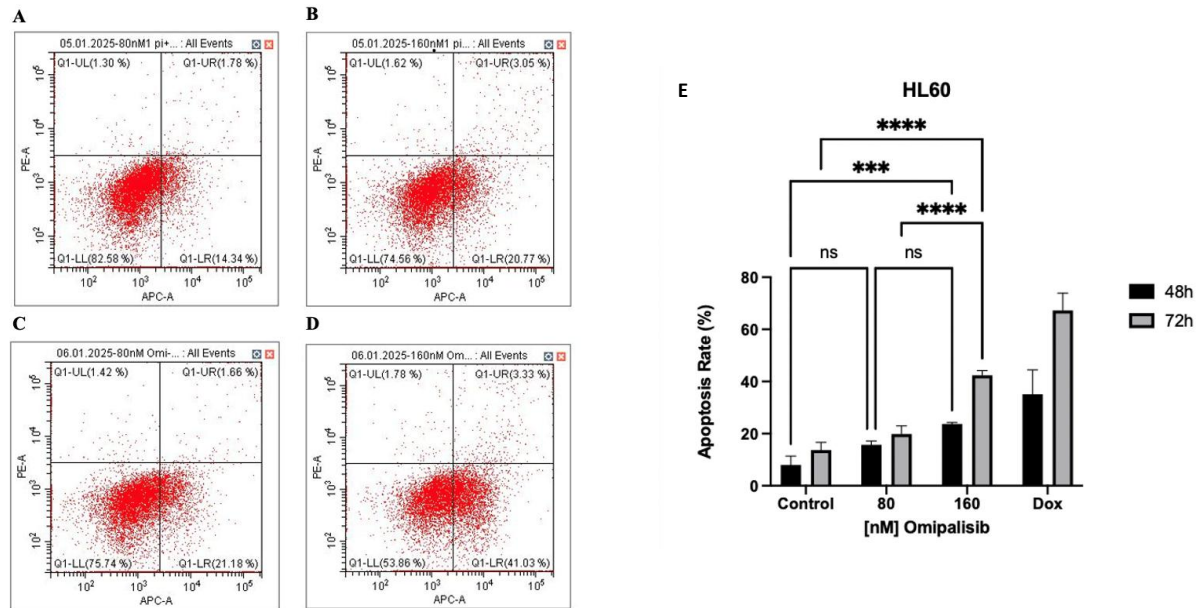


Figure 3. Flow cytometry analysis of apoptosis in HL60 cells treated with Omipalisib. Cells were treated with 80 nM and 160 nM Omipalisib for 48 or 72 hours, followed by Annexin V/PI staining A) 80nM Omipalisib for 48 hr, B) 160nM Omipalisib for 48 hr, C) 80nM Omipalisib for 72 hr, D) 160nM Omipalisib for 72 hr. The quadrants denote distinct cell populations: Q1-UL (necrotic cells), Q1-UR (late apoptotic cells), Q1-LL (live cells), and Q1-LR (early apoptotic cells). E) Apoptosis analysis of HL60 cells treated with Omipalisib for 48 and 72 hours, assessed by flow cytometry. Apoptotic cell percentages were determined using annexin V/PI staining. The data represent the mean \pm standard deviation (SD) from three independent experiments, with error bars denoting the standard deviation.

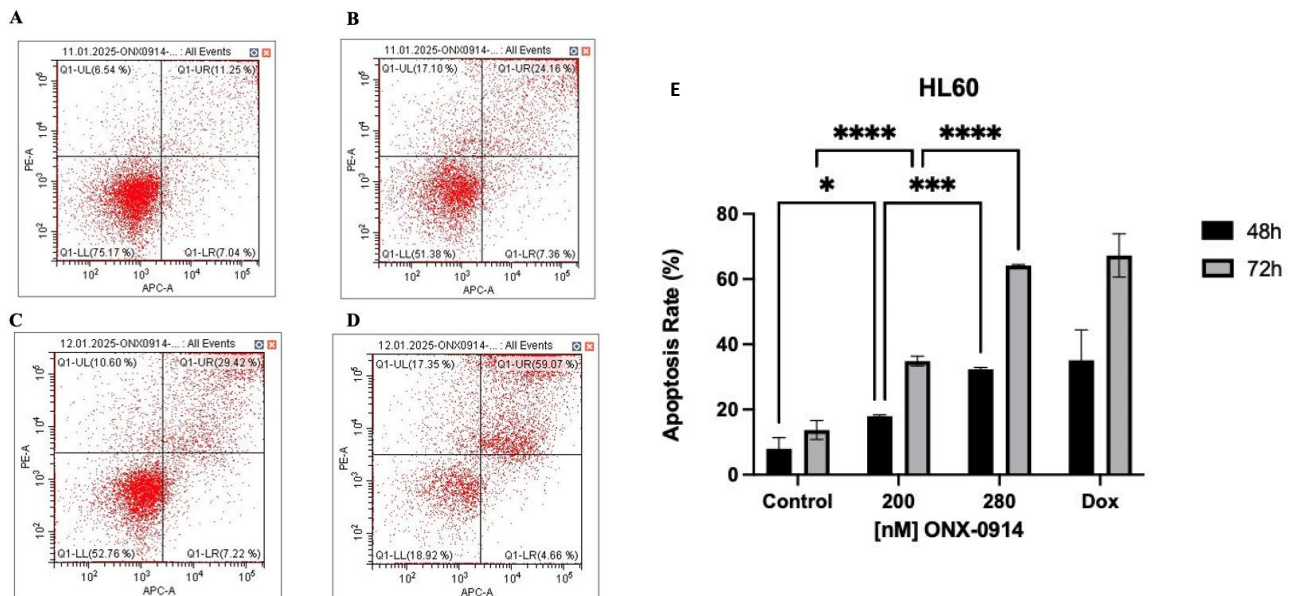


Figure 4. Flow cytometry analysis of apoptosis in HL60 cells treated with ONX-0914. Cells were treated with 200 nM and 280 nM Omipalisib for 48 or 72 hours, followed by Annexin V/PI staining A) 200nM ONX-0914 for 48 hr, B) 280 nM ONX-0914 for 48 hr, C) 200nM ONX-0914 for 72 hr, D) 280nM ONX-0914 for 72 hr. The quadrants denote distinct cell populations: Q1-UL (necrotic cells), Q1-UR (late apoptotic cells), Q1-LL (live cells), and Q1-LR (early apoptotic cells). E) Apoptosis analysis of HL60 cells treated with ONX-0914 for 48 and 72 hours, assessed by flow cytometry. Apoptotic cell percentages determined using annexin V/PI staining. Data represent the mean \pm standard deviation (SD) from three independent experiments. Error bars indicate standard deviation.

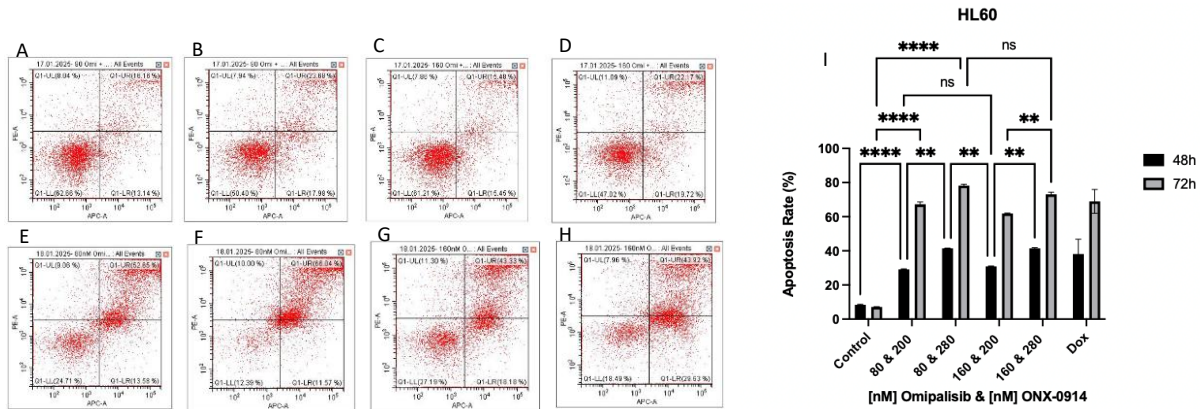


Figure 5. Flow cytometry analysis of apoptosis in HL60 cells treated with Omipalisib and ONX-0914 in combination. Cells treated with 200 and 280 nM Omipalisib for 48 hours, followed by Annexin V/PI staining A) 80nM Omipalisib & 200 nM ONX-0914, B) 80nM Omipalisib & 280 nM ONX-0914, C) 160nM Omipalisib & 200 nM ONX-0914, D) 160 Omipalisib & 280 nM ONX-0914. Flow cytometry analysis of apoptosis in HL60 cells treated with Omipalisib and ONX-0914 in combination. Cells treated with 200 and 280 nM Omipalisib for 72 hours, followed by Annexin V/PI staining E) 80nM Omipalisib & 200 nM ONX-0914, F) 80nM Omipalisib & 280 nM ONX-0914, G) 160nM Omipalisib & 200 nM ONX-0914, H) 160 Omipalisib & 280 nM ONX-0914. Apoptosis analysis of HL60 cells treated with Omipalisib and ONX-0914 for 48 and 72 hours, assessed by flow cytometry. Apoptotic cell percentages were determined using annexin V/PI staining. The data represent the mean \pm standard deviation (SD) from three independent experiments, with error bars denoting the standard deviation.

3.4 Western Blotting determines the Apoptotic Marker, Cleaved PARP Protein, on ONX-0914 and Omipalisib Treated HL60 Cells

In earlier chapters, we noted that both individual and combined therapies led to cell death in HL60 cells. Specifically, after assessing the percentage of apoptotic cells using flow cytometry, we intended to analyze the levels of cleaved PARP during apoptosis, along with β -actin as a loading control, concentrating on alterations noted during individual treatments. PARP-1 is generally present in a cell; however, it was observed that PARP-1 becomes cleaved by caspase-3 when cells go through apoptosis [27]. In this assay, the primary objective was to identify cells undergoing apoptosis because of PARP-1 for the single treatment at 48 hours.

The western blot analysis indicated that control cells do not exhibit any cleaved PARP-1; Doxorubicin was chosen as a positive control, resulting in a certain cell death. Doxorubicin revealed strong bands for cleaved PARP-1 in western blot analysis. At both concentrations of ONX-0914 (200nM and 280nM), cleaved PARP-1 was observed, and the band intensity increased with elevated concentrations of this agent. Additionally, PARP-1 cleavage was also observed, although not that significant with Omipalisib treatment at both 80nM and 160nM concentrations which suggests additional mechanisms being involved when cells undergo apoptosis by Omipalisib treatment (Figure 6).

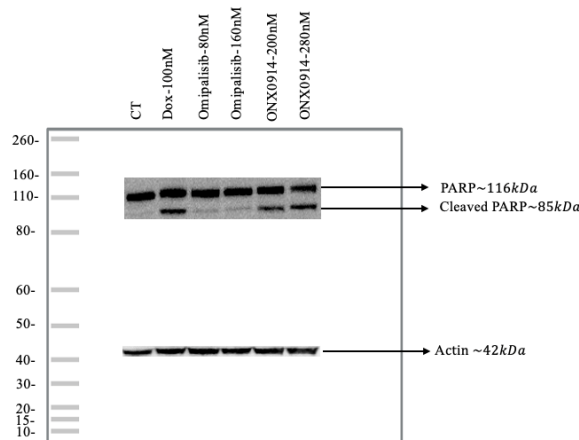


Figure 6. Apoptosis marker protein, cleaved Parp, detection assessed via western blot. HL60 cells treated with Omipalisib or ONX-0914 for 48 hours. Doxorubicin selected as positive control. The experiments repeated three times.

IV. CONCLUSION

In this study, we examined PSMB8 as a potential therapeutic target for Acute Myeloid Leukemia (AML) and assessed the possible efficacy of Omipalisib and ONX-0914 as treatment options. Our findings from in silico studies previously showed that PSMB8 is significantly overexpressed in AML patients and correlates with poorer survival outcomes, emphasizing its promise as a new target for drug development. Through in silico drug repurposing, we identified Omipalisib, a PI3K/mTOR inhibitor, as a promising candidate for AML treatment. Our in vitro analyses revealed that Omipalisib and ONX-0914 exert cytotoxic and pro-apoptotic effects on HL60 cells, with their impact varying according to concentration and exposure duration. Furthermore, combination therapy enhanced cell death more effectively than individual therapies, suggesting a synergistic effect that may help overcome drug resistance in aggressive AML subtypes. These findings lay a solid groundwork for future research on targeting PSMB8 in AML and highlight the importance of further preclinical and clinical evaluations to confirm the therapeutic potential of these inhibitors, particularly in more aggressive AML subtypes, such as those with FLT3 mutations and other chromosomal abnormalities.

ACKNOWLEDGEMENT

This study is completed as a part of Master Thesis submitted to İzmir University of Economics, Graduate School, Master's Program in Bioengineering by Onur Ateş in 2025. The authors thank TUBITAK ULAKBIM, High Performance and Grid Computing Center (TRUBA resources) for the calculations by their computational resources used to led this study.

REFERENCES

- [1] Pelcovits, A., & Niroula, R. (2020). Acute Myeloid Leukemia: A Review. *103*(3), 38-40.
- [2] Kishtagari, A., Levine, R. L., & Viny, A. D. (2020). Driver mutations in acute myeloid leukemia. *27*(2), 49-57.
- [3] Döhner, H., Weisdorf, D. J., & Bloomfield, C. D. (2015). Acute Myeloid Leukemia. *The New England Journal of Medicine*, *373*(12), 1136–1152.
- [4] Vosberg, S., & Greif, P. A. (2019). Clonal evolution of acute myeloid leukemia from diagnosis to relapse. *Genes, Chromosomes & Cancer*, *58*(12), 839–849.
- [5] Xu, J., & Niu, T. (2020). Natural killer cell-based immunotherapy for acute myeloid leukemia. *Journal of Hematology & Oncology* *2020* *13*:1, *13*(1), 1–20.
- [6] DiNardo, C. D., Erba, H. P., Freeman, S. D., & Wei, A. H. (2023). Acute myeloid leukaemia. *The Lancet*, *401*(10393), 2073–2086.
- [7] Kloetzel, P. M. (2001). Antigen processing by the proteasome. *Nature Reviews. Molecular Cell Biology*, *2*(3), 179–187.
- [8] Murata, S., Yashiroda, H., & Tanaka, K. (2009). Molecular mechanisms of proteasome assembly. *Nature Reviews. Molecular Cell Biology*, *10*(2), 104–115.
- [9] Rivett, A. J., & Hearn, A. R. (2004). Proteasome function in antigen presentation: immunoproteasome complexes, Peptide production, and interactions with viral proteins. *Current Protein & Peptide Science*, *5*(3), 153–161.
- [10] Kimura, H., Caturegli, P., Takahashi, M., & Suzuki, K. (2015). New Insights into the Function of the Immunoproteasome in Immune and Nonimmune Cells. *Journal of Immunology Research*, 2015.
- [11] Lai, C., Doucette, K., & Norsworthy, K. (2019). Recent drug approvals for acute myeloid leukemia. *Journal of Hematology and Oncology*, *12*(1), 1–20.
- [12] Agarwal, A. K., Xing, C., Demartino, G. N., Mizrachi, D., Hernandez, M. D., Sousa, A. B., Martínez De Villarreal, L., Dos Santos, H. G., & Garg, A. (2010). PSMB8 Encoding the $\beta 5i$ Proteasome Subunit Is Mutated in Joint Contractures, Muscle Atrophy, Microcytic Anemia, and Panniculitis-Induced Lipodystrophy Syndrome. *American Journal of Human Genetics*, *87*(6), 866.
- [13] Chang, H. H., Cheng, Y. C., Tsai, W. C., & Chen, Y. (2020). PSMB8 inhibition decreases tumor angiogenesis in glioblastoma through vascular endothelial growth factor A reduction. *Cancer Science*, *111*(11), 4142–4153.
- [14] Zhang, Y., Xue, S., Hao, Q., Liu, F., Huang, W., & Wang, J. (2021). Galectin-9 and PSMB8 overexpression predict unfavorable prognosis in patients with AML. *Journal of Cancer*, *12*(14), 4257–4263.
- [15] Lei, M., Jingjing, Z., Tao, J., Jianping, M., Yuanxin, Z., Jifeng, W., Lianguo, X., Lidong, Z., & Ying, W. (2020). LncRNA HCP5 promotes LAML progression via PSMB8-mediated PI3K/AKT pathway activation. *Naunyn-Schmiedeberg's Archives of Pharmacology*, *393*(6), 1025–1032.
- [16] Tükel, E. Y., Ateş, O., & Kiraz, Y. (2024). In Silico Drug Repurposing Against PSMB8 as a Potential Target for Acute Myeloid Leukemia Treatment. *Molecular Biotechnology*, 1–11.
- [17] Tang, Z., Li, C., Kang, B., Gao, G., Li, C., & Zhang, Z. (2017). GEPIA: a web server for cancer and normal gene expression profiling and interactive analyses. *Nucleic Acids Research*, *45*(W1), W98–W102.
- [18] Corsello, S. M., Bittker, J. A., Liu, Z., Gould, J., McCarren, P., Hirschman, J. E., Johnston, S. E., Vrcic, A., Wong, B., Khan, M., Asiedu, J., Narayan, R., Mader, C. C., Subramanian, A., & Golub, T. R. (2017). The Drug Repurposing Hub: a next-generation drug library and information resource. *Nature Medicine*, *23*(4), 405–408.

- [19] Sleire, L., Førde-Tislevoll, H. E., Netland, I. A., Leiss, L., Skeie, B. S., & Enger, P. Ø. (2017). Drug repurposing in cancer. *Pharmacological Research*, 124, 74–91.
- [20] Xue, H., Li, J., Xie, H., & Wang, Y. (2018). Review of Drug Repositioning Approaches and Resources. *International Journal of Biological Sciences*, 14(10), 1232.
- [21] Darici, S., Alkhaldi, H., Horne, G., Jørgensen, H. G., Marmiroli, S., & Huang, X. (2020). Targeting PI3K/Akt/mTOR in AML: Rationale and Clinical Evidence. *Journal of Clinical Medicine*, 9(9), 2934.
- [22] Maciej Serda, Becker, F. G., Cleary, M., Team, R. M., Holtermann, H., The, D., Agenda, N., Science, P., Sk, S. K., Hinnebusch, R., Hinnebusch A, R., Rabinovich, I., Olmert, Y., Uld, D. Q. G. L. Q., Ri, W. K. H. U., Lq, V., Frxqw, W. K. H., Zklfk, E., Edvhg, L. V. (2012). Enalapril-induced Apoptosis of Acute Promyelocytic Leukaemia Cells Involves STAT5A. *ANTICANCER RESEARCH*, 32(7), 343–354.
- [23] Fan, Y., Chiu, J. F., Liu, J., Deng, Y., Xu, C., Zhang, J., & Li, G. (2018). Resveratrol induces autophagy-dependent apoptosis in HL-60 cells. *BMC Cancer*, 18(1), 1–10
- [24] Jenkins, T. W., Downey-Kopyscinski, S. L., Fields, J. L., Rahme, G. J., Colley, W. C., Israel, M. A., Maksimenko, A. V., Fiering, S. N., & Kisselev, A. F. (2021). Activity of immunoproteasome inhibitor ONX-0914 in acute lymphoblastic leukemia expressing MLL–AF4 fusion protein. *Scientific Reports*, 11(1), 10883.
- [25] Lakshmanan, I., & Batra, S. K. (2013). Protocol for Apoptosis Assay by Flow Cytometry Using Annexin V Staining Method. *Bio-Protocol*, 3(6), e374.
- [26] Petsri, K., Yokoya, M., Tungsukruthai, S., Rungrotmongkol, T., Nutho, B., Vinayanuwattikun, C., Saito, N., Takehiro, M., Sato, R., & Chanvorachote, P. (2020). Structure–Activity Relationships and Molecular Docking Analysis of Mcl-1 Targeting Renieramycin T Analogues in Patient-derived Lung Cancer Cells. *Cancers*, 12(4), 875
- [27] Ordueri, N. E. G., Elgün, T., Şahin, P., Kuşcu, N., & Özenci, Ç. Ç. (2018). Postnatal fare testis gelişiminde kaspaz-bağımlı ve kaspaz-bağımsız apoptozun değerlendirilmesi. *Uludağ Üniversitesi Tıp Fakültesi Dergisi*, 44(2), 103–109.